Journal of Applied Physics ARTICLE scitation.org/journal/jap

Effects of fast and thermal neutron irradiation on Ga-polar and N-polar GaN diodes

Cite as: J. Appl. Phys. 133, 015704 (2023); doi: 10.1063/5.0119294
Submitted: 8 August 2022 · Accepted: 1 December 2022 ·
Published Online: 5 January 2023

F. Mirkhosravi,[1,a)] A. Rashidi,[1] A. T. Elshafiey,[1] J. Gallagher,[2] Z. Abedi,[3] K. Ahn,[4] A. Lintereur,[2] E. K. Mace,[5] M. A. Scarpulla,[4,6] and D. Feezell[1,3,a)]

AFFILIATIONS

[1]Center for High Technology Materials (CHTM), University of New Mexico, Albuquerque, New Mexico, 87106 USA
[2]Nuclear Engineering, Pennsylvania State University, University Park, Pennsylvania 16802, USA
[3]Electrical and Computer Engineering, University of New Mexico, Albuquerque, New Mexico 87106, USA
[4]Electrical and Computer Engineering, University of Utah, Salt Lake City, Utah 84112, USA
[5]Pacific Northwest National Laboratory, Richland, Washington 99254, USA
[6]Material Science and Engineering, University of Utah, Salt Lake City, Utah 84112, USA

Note: This paper is part of the Special Topic on Radiation Effects in Materials.
[a)]**Authors to whom correspondence should be addressed:** Fmirkhosravi@unm.edu and dfeezell@unm.edu

ABSTRACT

Studies of the radiation tolerance and electrical behavior of gallium nitride (GaN) based devices are important for the next generation of high-power and high-voltage electronics that may be subjected to harsh environments such as nuclear reactor and fusion facilities, particle accelerators, and post-denotation environments. In this work, we study the behavior of Ga-polar and N-polar GaN Schottky diodes before and after exposure to fast and thermal + fast neutrons. Temperature-dependent current–voltage (I–V) and circular transmission line method (CTLM) measurements were used to study the electrical characteristics. A strong reduction in reverse leakage current and an increase in differential resistance in forward bias were observed after neutron irradiation. Thermionic emission (TE), Frenkel–Poole (FP) emission, and Fowler–Nordheim (FN) tunneling models were used to explain the forward and reverse I–V characteristics pre- and post-irradiation. The study confirms that Ga-polar and N-polar GaN Schottky diodes exhibit different electrical responses to fast and thermal neutron irradiations. The reverse bias characteristics of N-polar diodes are less affected after the fast neutron irradiation compared to Ga-polar diodes, while in the forward bias region, the electrical behavior after fast and thermal neutron irradiations is similar in Ga-polar and N-polar diodes. The results indicate that the role of orientation should be considered in the design of GaN-based radiation-tolerant electronics.

I. INTRODUCTION

GaN-based materials have well-known applications in high electron mobility transistors (HEMTs), power electronics, and optoelectronic devices. GaN-based materials are also attractive for use in environments with high levels of radiation exposure[1–3] due to their high mechanical, thermal, and chemical stability.[4,5] The higher displacement energy of Ga and N atoms in GaN crystals provides higher resistance than Si, GaAs, and SiC to various types of radiations.[6,7]

Out of common types of radiations, a high-flux neutron radiation is particularly relevant to the development of radiation-tolerant electronics due to its presence in nuclear reactor and fusion facilities, particle accelerators, post-detonation environments, and aerospace applications.[8] The neutron irradiation results in atomic displacements in the lattice, including the creation of vacancies, interstitials, Frenkel–Poole defects, and Gossick zones.[3,9–11] It was also demonstrated that radiation-induced defect production rates are dependent on the initial density and types of pre-existing defects in the material.[12] Previous reports have confirmed that the neutron irradiation also significantly affects device performance through atomic displacements, the creation of deep levels and recombination centers, and damage to the contacts.[7,8,13,14] A variety of changes to the electrical behavior of GaN-based devices have been reported in the literature. A shift in

threshold voltage and a decrease in 2DEG mobility was previously observed in neutron irradiated HEMT structures.[15–17] An increase in the density of acceptor states and a decrease in Schottky diode capacitance in the accumulation region were also reported.[18] Carrier removal from trapping at defect centers induced by radiation resulted in a decrease in capacitance in capacitance–voltage (C–V) characteristics. Depending on the energy of the particles, neutron fluence is usually described as fast (above 1 eV) or thermal (below 1 eV). Fast neutrons are more responsible for creating an insulating phase and recombination centers that increase the diode ideality factor and lower the carrier transport in Schottky diodes, while thermal neutrons can cause an annealing effect at the GaN/metal interface that at lower fluences may improve the device performance by reduction in the ideality factor.[8] Degradation in *I–V* characteristics and optical properties corresponding to irradiation fluences and at different ratios of the fast/thermal neutron irradiation have been reported.[19,20] Similar effects in other GaN-based devices, such as light-emitting diodes (LEDs),[13] Schottky diodes,[8,18] and GaN radiation detectors,[7] were also observed.

Although there have been a variety of neutron irradiation studies performed on Ga-polar GaN-based devices, to the best of our knowledge, there have been no studies to date on N-polar GaN-based devices. N-polar GaN is attractive for its potential advantages in both electronic and optoelectronic devices, including HEMTs, LEDs, and solar cells.[21–23] In HEMTs, the re-ordering of the GaN and AlGaN layers enables access to the two-dimensional electron gas (2DEG) through GaN, resulting in lower ohmic contact resistance.[24] In LEDs, enhanced injection and collection efficiency are possible[25,26] and the higher thermal stability of N-polar indium nitride may be attractive.[27,28] The Ga-polar and N-polar orientations are expected to respond differently to the neutron irradiation due to their opposite polarity and different pre-irradiation defect profiles.

In this work, we study the effects of fast and thermal neutron irradiations on n-type GaN Schottky diodes on both Ga-polar and N-polar orientations using temperature-dependent current–voltage (*I–V*) and circular transmission line measurements (CTLMs). Both fast and thermal neutrons are included in the study to capture the effects of the different particle fluence energies of these species. Modeling based on the thermionic emission (TE), Frenkel–Poole (FP) emission, and Fowler–Nordheim (FN) tunneling is used to explain the electrical behavior of the Ga-polar and N-polar Schottky diodes pre- and post-fast and thermal + fast neutron irradiations in both forward and reverse bias regions.

II. SCHOTTKY DIODE TEST STRUCTURE AND CHARACTERIZATION

Ga-polar and N-polar Schottky diodes were grown in a Veeco P-75 rotating TurboDisc metal-organic chemical-vapor deposition (MOCVD) system and fabricated using a similar approach to what was previously reported.[29] A sapphire substrate with a 4° miscut toward the *a*-plane was used for the N-polar growth to achieve smooth surface morphology. The Schottky diode structures on both orientations include 2 μm of unintentionally doped (UID) GaN, 200 nm of highly doped *n*-type GaN (n^{++} GaN) with a silicon concentration of 8×10^{18} cm^{-3}, and a 700 nm drift layer with a silicon concentration of $\sim 4 \times 10^{16}$ cm^{-3}. Pd/Au (20/300 nm) was used to form the Schottky contact, and Cr/Au (20/600 nm) was used as the ohmic contact. The ohmic contact was annealed at 500 °C for 40 s in nitrogen ambient. These metals were chosen based on their contact properties and to minimize post-irradiation activation. CTLM pads were also deposited on the n^{++} layer using the same metallization scheme used for the contacts. Devices with diameters of 150 μm were fabricated on these samples. A schematic image of the Schottky diode structure is shown in Fig. 1.

Neutron irradiations were performed at the Pennsylvania State University (PSU) Breazeale Reactor, a 1 MW TRIGA reactor with a moveable core in a large pool, using a fast neutron irradiator (FNI) and a dry tube. The neutron energies are typical of a fission spectrum, where energies range from 10^{-10} to ~20 MeV. The FNI provided an approximately 1:550 thermal:fast neutron flux profile, and the dry tube provided an approximately 2:1 thermal:fast flux. The FNI neutrons peak at 1 MeV with an average energy of 0.85 MeV, and almost 83% of the FNI neutrons have energies above 0.1 MeV. The thermal neutron energies peak at 0.0253 eV. A cutoff energy of 1 eV was defined for the purpose of calculating the thermal:fast ratios (Table I). Technically speaking, neutrons in the range of 1 eV–0.1 MeV are typically considered epithermal neutrons and energies above 0.1 MeV are fast neutrons. Samples were irradiated to three different FNI fluences (10^{10}, 10^{14}, and 10^{16} n/cm^2) and to 10^{16} n/cm^2 in the dry tube. For simplicity, we refer to the FNI irradiations as *fast*, and the dry tube irradiations as *thermal + fast* for the rest of the paper. The times required to achieve these fluences ranged from a couple of minutes to several hours. After irradiation, the samples cooled for nearly two months prior to shipping and post-irradiation characterization. The two-month cooldown time was necessary for the samples to reach a radiation level below 0.5 mR/h, as required by UNM radiation safety policies. Kim *et al.* reported almost full recovery of their samples after the neutron irradiation up to 10^{11} n/cm^2 fluence after 18 days in HEMT structures due to the self-healing mechanism of point defects.[30] However, we note that the maximum neutron fluence in the present work is five orders of magnitude higher than that reported by Kim *et al.* Even though some transient effects may have recovered during this two-month period, the samples show significant permanent damage that is stable over time. For example, the post-irradiation *I–V* characteristics obtained after two-months are very similar to the post-irradiation *I–V* characteristics obtained after one

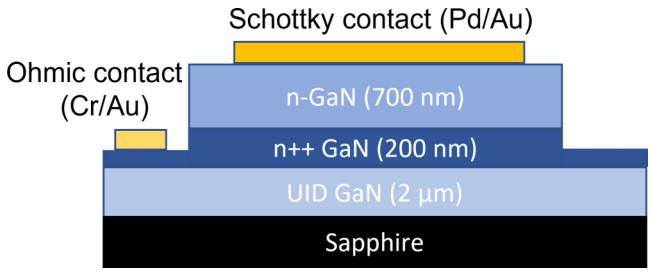

FIG. 1. Schematic image of the Schottky diode structure on both Ga-polar and N-polar orientations.

year. The forward I–V characteristics are indistinguishable, while the reverse characteristics show only slight recovery (~10% for N-polar and ~2% for Ga-polar diodes) after almost one year of storing the samples at room temperature.

III. RESULTS AND DISCUSSION

Room-temperature I–V, CTLM, and temperature dependent I–V measurements were made on each diode before and after irradiation to study and quantify the major differences between Ga-polar and N-polar diodes, and to compare the effects between fast and thermal + fast neutron irradiations. The data were collected from devices with 150 μm diameters and a four-wire probe configuration was used to eliminate probe and line resistances in the I–V measurement system.

Representative linear and logarithmic I–V curves for Ga-polar and N-polar n-type Schottky diodes are shown in Figs. 2 and 3, respectively. The Ga-polar diodes (Fig. 2) show a fluence-dependent reduction in reverse leakage current. For fast neutron fluences of 10^{10} and 10^{14} n/cm^2, the post-irradiation leakage is 0.3 times the pre-irradiation leakage, and for a fluence of 10^{16} n/cm^2, the post-irradiation leakage is 0.009 times the pre-irradiation leakage, both measured at −8 V. For the thermal + fast neutron irradiation (fluence of 10^{16} n/cm^2), the reduction in reverse leakage current is about 0.02 times the pre-irradiation leakage at −8 V and is less than the reduction in leakage for the 10^{16} n/cm^2 fluence of fast neutrons. Also, all irradiated devices show a shift to the left in the minimum current away from V = 0 in the post-irradiation I–V characteristics. The shift in the minimum current is related to positive charge trapping after irradiation.[8] For the fluence of 10^{16} n/cm^2, both fast and thermal + fast neutron irradiations result in an increase in the differential resistance of the Schottky diode, as shown in the linear I–V insets.

The I–V behaviors of the N-polar Schottky diodes are slightly different from the Ga-polar diodes, as shown in Fig. 3. There is very little change in the I–V characteristics for the 10^{10} n/cm^2 fluence of fast neutrons in the N-polar diodes. A reduction in the reverse leakage current at −8 V appears at 10^{14} n/cm^2 (0.42 times the pre-irradiation) and 10^{16} n/cm^2 (0.052 time the pre-irradiation) fluences of fast neutrons, while at the 1×10^{16} n/cm^2 fluence of the thermal + fast neutron irradiation, the changes in the reverse leakage current at higher bias voltages are negligible, and only a slight increase is shown at lower bias voltages [Fig. 3(d)]. The changes in differential resistance in the forward region are similar to the changes observed in the Ga-polar Schottky diodes. However, unlike the Ga-polar Schottky diodes, there is no shift in the minimum current position after irradiation. Figure 4 shows the post-irradiation I–V sweeps in the range −8 to +3 V in both forward and reverse sweep directions with 10^{16} n/cm^2 fast neutrons for the Ga-polar and N-polar samples, showing that the shift in minimum current position relative to minimum at 0 V, as shown in Figs. 2 and 3, depends on the sweep direction. For the Ga-polar device [Fig. 4(a)], there is almost no shift in minimum current when the device is swept from positive to negative voltage, but there is a 1 V reduction in the minimum current position when the device is swept from negative to positive. For the N-polar device [Fig. 4(b)], the opposite trend is observed and there is no shift in minimum current when the device is swept from negative to positive voltage, but a slight shift to the right appears in the positive to negative sweep. This hysteresis behavior in the low bias voltages in both the reverse and forward regions is explained by the population or de-population of surface states or trap states, which are affected by the direction of the applied electric field and internal spontaneous polarization field. The surface composition and chemical treatment,[31] along with the effect of GaN orientation on Schottky barrier height,[32] can also affect the I–V hysteresis behavior. The opposite polarization field in Ga-polar and N-polar is known to result in the accumulation of opposite charge at surface states.[33–35] A negative to positive sweep will trap additional positive charges in Ga-polar samples, while for the N-polar samples, a negative to positive sweep will trap additional negative charges. Thus, when the applied external field is aligned with the internal spontaneous polarization field, it will result in more accumulation of charge, but when it is in the opposite direction, it will empty the accumulated charge. This accumulated charge would contribute to the I–V behavior as a capacitive current that may release at a certain bias voltage in the opposite direction. Note that this hysteresis appears after irradiation, indicating that a higher density of trap states is available after the neutron irradiation. The creation of new defect centers or re-orientation of existing defects and dislocation states in the bulk and at the surface should result in an increase in the charge trap density in defect states.

Temperature-dependent I–V measurements (from 303 to 423 K) were performed on both the fast and thermal + fast neutron irradiated samples, as well as on un-irradiated Ga-polar and N-polar diodes. The temperature-dependent I–V characteristics were used to extract the ideality factor and Schottky barrier height (SBH) pre- and post-irradiation. In the following analysis, the thermionic emission is assumed to be the dominant carrier transport mechanism in the forward bias region in the Schottky diodes and the forward current density can be described by the following equation:

$$J_{TE} = A^{*}T^{2}\exp\left(-\frac{q\varphi_b}{kT}\right)\left\{\exp\left(\frac{qV - Ir_s}{nkT}\right) - 1\right\}, \quad (1)$$

where $J_{TE} = I_{TE}/Area$ and is the current density corresponding to the thermionic emission, A^{*} is the effective Richardson constant, T is the temperature in kelvin, q is the electron charge, φ_b is the SBH, n is the ideality factor, k is the Boltzmann constant, and r_s is the series resistance. r_s is important for the higher forward bias region after turn-on, while for the lower forward bias region, a pure thermionic emission is assumed. A plot of $\ln(J_{TE})$ vs V for the low forward bias region shows a linear behavior (not shown here),

TABLE I. Neutron energy characteristics of the FNI and the dry tube.

	Min (MeV)	Max (MeV)	Peak (MeV)	Ratio (thermal:fast)
FNI	10^{-10}	20	1	1:550
Dry tube	10^{-10}	20	0.0253	2:1

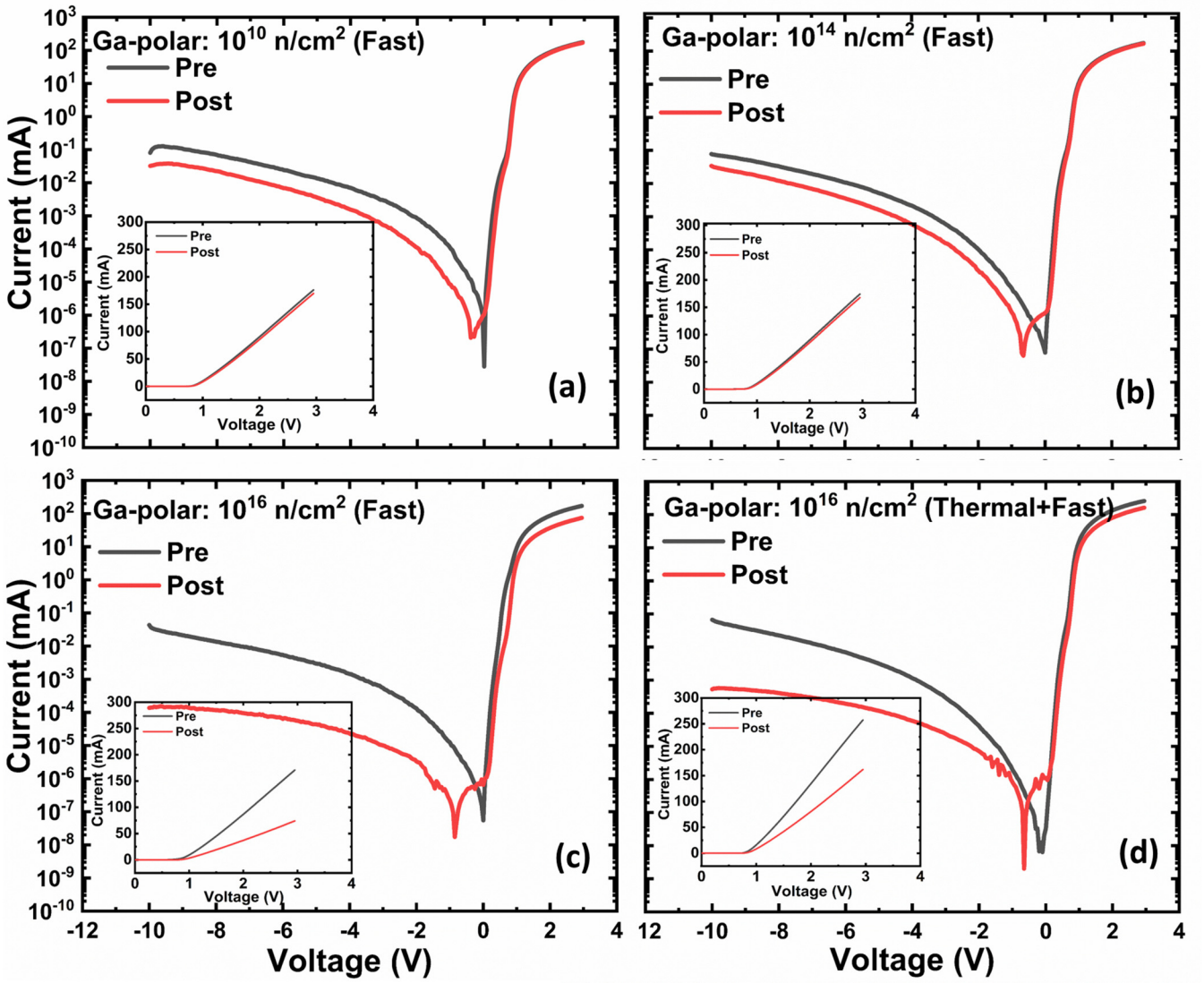

FIG. 2. Pre- and post-irradiation Ga-polar n-type Schottky diode *I–V* curves[(a)–(d) for 10^{10}, 10^{14}, 10^{16} fast, and 10^{16} thermal + fast, respectively]. Note that the reduction in reverse leakage current is more significant for higher fluences, and at the highest fluences, 10^{16} n/cm^2, there is also an increase in the differential resistance of the Schottky diode, for both the fast neutron fluence and the thermal + fast neutron fluence.

where $J_{total} \approx J_{TE}$, and the series resistance is negligible. The ideality factor and the SBH can be extracted from the slope and intercept of the plot, respectively. Figure 5 shows the extracted ideality factor [Fig. 5(a)] and barrier height [Fig. 5(b)] at different temperatures (from 303 to 423 K) for Ga-polar (black) and N-polar (green) Schottky diodes. For Ga-polar diodes, the ideality factor shows relatively constant behavior at different temperatures and increases after both fast and thermal + fast neutron irradiations. The low temperature dependence of the ideality factor in the Ga-polar diodes (which has often been observed experimentally) can be explained by an inhomogeneous SBH in which current transport is dominant through the low-SBH regions.[36] The SBH increases with temperature in all cases, suggesting the existence of laterally extended SBH inhomogeneities at the metal–semiconductor interface.[37] While the trends in the ideality factor and SBH are almost the same before and after neutron irradiations, on the Ga-polar diodes, we observe a larger increase in the ideality factor with the fast neutron irradiation. The increase in the ideality factor is an indication of new neutron-induced defects, and the increase is larger for the fast neutron case, which is consistent with the higher atomic displacement probability compared to thermal + fast neutrons [Fig. 5(a)]. The SBH, on the other hand, shows the most

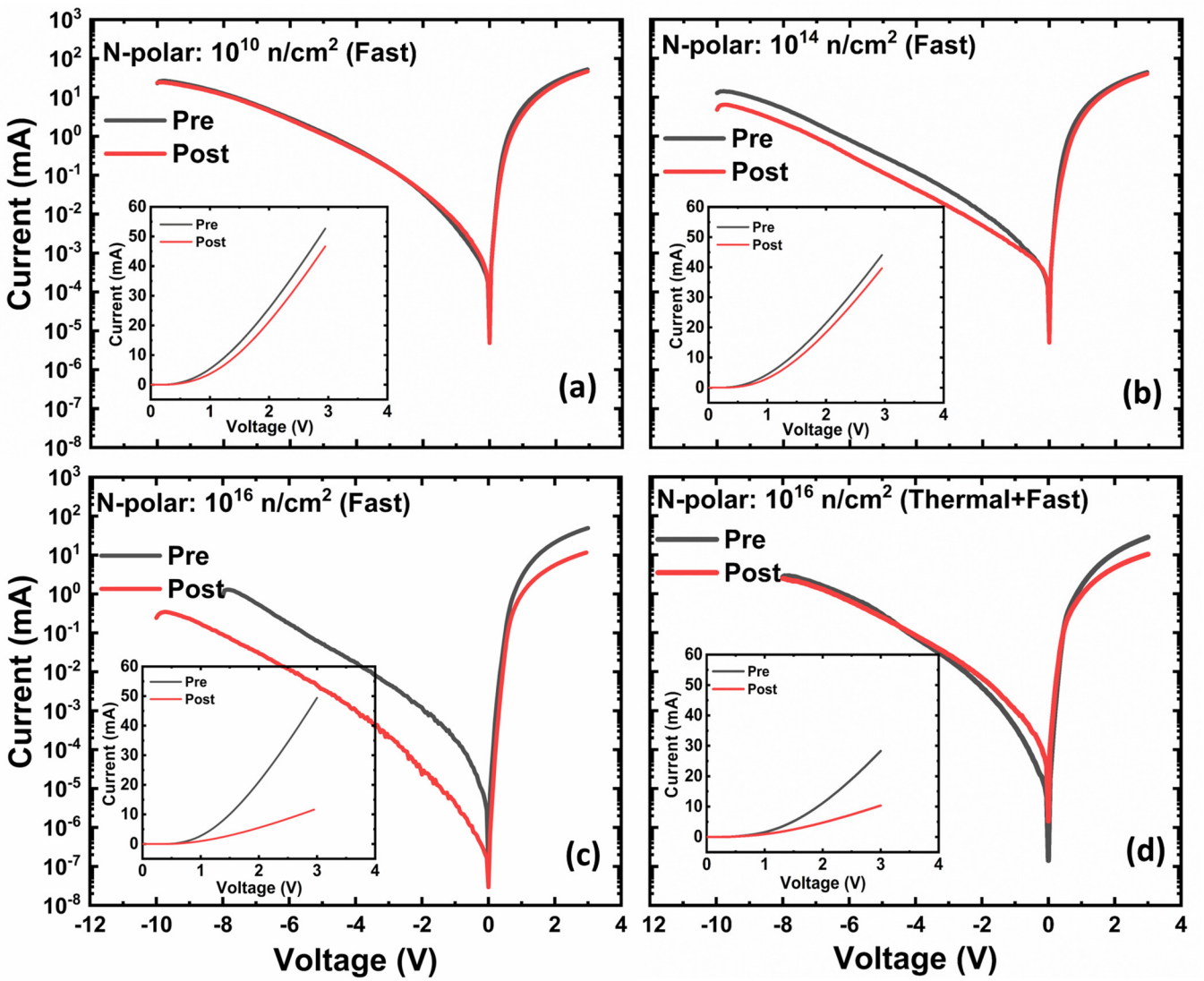

FIG. 3. Pre- and post-irradiation N-polar n-type Schottky diode IV curves [(a)–(d) for 10^{10}, 10^{14}, 10^{16} fast, and 10^{16} thermal + fast, respectively]. Note that there is a less change in the differential resistance of the Schottky diode when irradiated with the predominately thermal fluence compared to the predominately fast fluence.

increase after the thermal + fast neutron irradiation [Fig. 5(b)], suggesting that the annealing effect from thermal neutrons could be more detrimental to the metal/GaN interface.

In the N-polar diode, we observed a different trend in the temperature dependence of the ideality factor. The ideality factor increases with decreasing temperature, indicating that the thermionic emission becomes less dominant at low temperatures and suggesting that the thermionic field emission (TFE) may also contribute to the current at low temperatures. Generally speaking, the deviation of the ideality factor from unity (i.e., pure thermionic emission) has been attributed to image-force lowering, generation-recombination, interface states, and tunneling.[36] These phenomena are all directly altered by fast and thermal neutron irradiations and directly affect the ideality factor and SBH. Contrary to the Ga-polar diodes, the ideality factor in the N-polar diodes increases significantly at lower temperatures with the thermal + fast neutron irradiation and at higher temperatures with the fast neutron irradiation. Also, the range of the variation with temperature is larger in the thermal + fast case, which could be related to further deviation from the pure thermionic emission in N-polar diodes after irradiation compared to Ga-polar diodes. The SBH on the N-polar diodes increases with the fast neutron irradiation over the full range of temperatures. For the thermal + fast irradiation, there was a minimal change at lower temperatures and a moderate increase at higher temperatures. We also

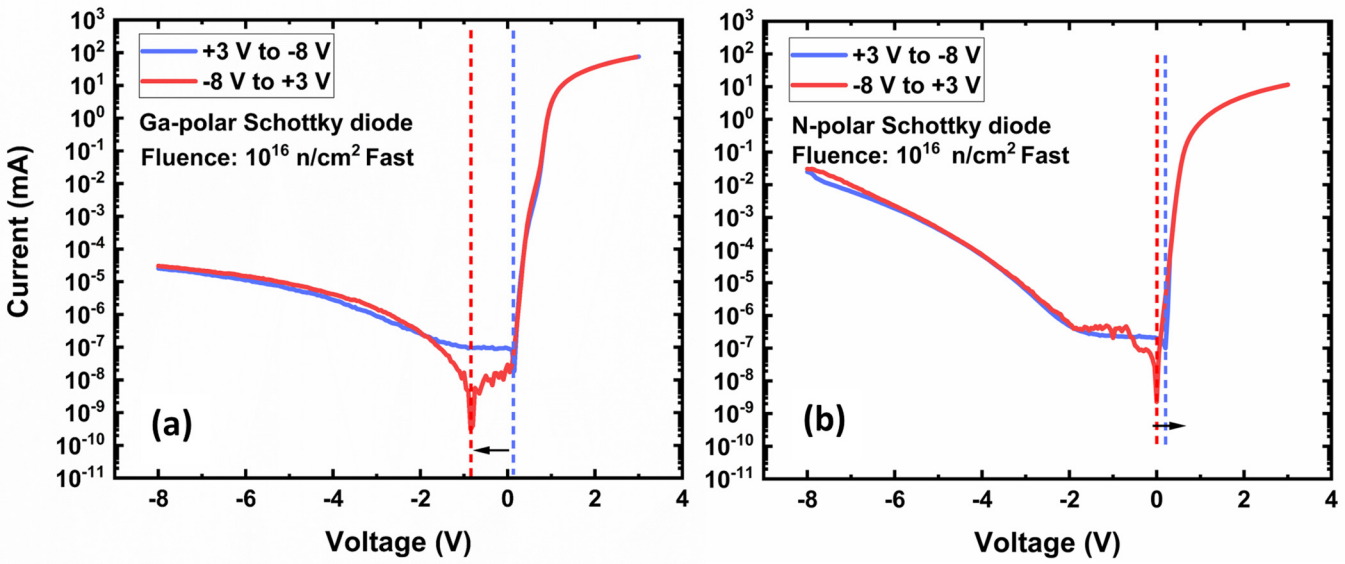

FIG. 4. Shift in the minimum current position relative to 0 V in *I–V* after irradiation on the highest fluence of the fast neutron irradiation depending on the sweep direction. Shifts appear for Ga-polar devices (a) when they are swept from negative to positive and for N-polar devices (b) when they are swept from positive to negative.

note that there is almost no recovery, especially in the forward bias region, due to annealing the samples up to 423 K during this measurement, as the measured *I–V* after annealing has the same characteristics compared to before annealing.

Series resistance can be extracted from the higher forward bias region using the following equation:[38]

$$\frac{I}{g_d} = Ir_s + \frac{nkT}{q}, \tag{2}$$

where $g_d = dI/dV$ is the diode differential conductance at voltages where r_s is important. From the slope of the I/g_d vs I plot, the series resistance of the diode can be extracted. For the two lower

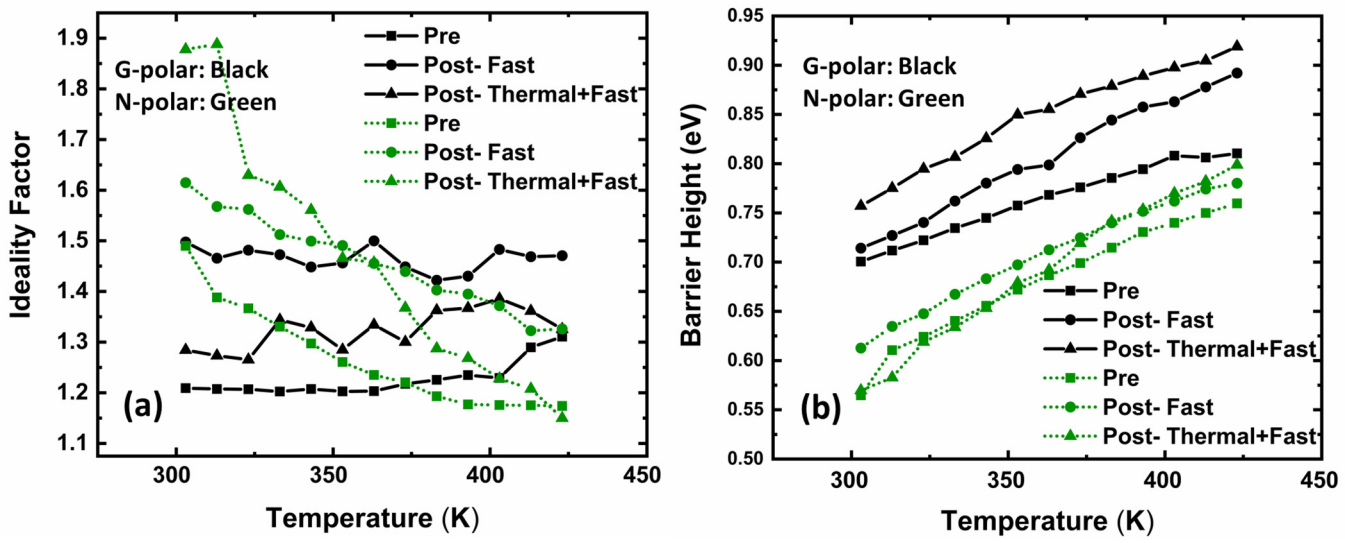

FIG. 5. Ideality factor (a) and Schottky barrier height (b) extracted from the TE model for Ga-polar (black) and N-polar (green) pre- and post-irradiation for fast and thermal + fast neutrons.

fluences (10^{10} and 10^{14} n/cm^2) of the fast neutron irradiation, there are no significant changes in r_s in either the Ga-polar or the N-polar diodes. For the highest fluence (10^{16} n/cm^2) of the fast neutron irradiation, there is almost a 120% increase (from 10.8 to 23.7 Ω) in the series resistance in the Ga-polar diodes and a 330% increase (from 28.0 to 120.3 Ω) for the N-polar diodes. In the case of the thermal + fast (10^{16} n/cm^2) neutron irradiation, there is only a 42% increase (from 7.6 to 10.8 Ω) in the Ga-polar diodes, but there is a 223% increase (from 40.7 to 131.4 Ω) in the N-polar diodes.

The resistivity and specific contact resistance of the ohmic contacts on the Ga-polar and N-polar diodes were studied using CTLM measurements pre- and post-irradiation. The technique we used for this study, and the analysis approach, has been discussed in an earlier publication.[29] Figure 6(a) shows the resistivity for the Ga-polar samples pre- and post-irradiation. The resistivity increased for the samples exposed to fast neutrons, while the sample exposed to thermal + fast neutrons showed no change in resistivity. The increase in resistivity for the fast neutron irradiation is related to displacement damage in the GaN crystal. However, the change in specific contact resistance [Fig. 6(b)] for the fast neutron irradiation is lower than that observed for the thermal + fast neutron irradiation. These results are in agreement with previous studies on Ga-polar devices, which indicated that fast neutrons are more responsible for changes to the bulk material and thermal neutrons affect the contact.[8]

The N-polar sample, as shown in Fig. 7, depicts a similar pattern for the fast neutron irradiation effects; there is a small increase for the two lower fluences, and a much larger increase for the highest fast neutron fluence. Unlike the behavior of the Ga-polar sample, the N-polar samples show nearly the same increase in resistivity for the thermal + fast neutron irradiation and the highest fluence of the fast neutron irradiation. This suggests that despite the low ratio (1:2) of fast neutrons compared to thermal neutrons in the thermal + fast case, there is still some lattice disorder damage on the N-polar orientation. Regarding the specific contact resistance, while a significant increase was observed only in the thermal + fast neutron case on the Ga-polar samples, the N-polar samples showed an increase in specific contact resistance for the 10^{16} n/cm^2 fluence of both the fast and thermal + fast neutron irradiations. The series resistance is affected by both the bulk resistivity and the specific contact resistance. The CTLM results agree with the observed increase in series resistance extracted from the *I–V* data for both the Ga-polar and N-polar diodes.

Temperature-dependent *I–V* characteristics were also measured in the reverse bias region to −8 V. The temperature-dependent reverse *I–V* and current density (inset) vs temperature at different voltages for pre-irradiation and for fast and thermal + fast with 10^{16} n/cm^2 fluence are shown in Fig. 8. Before irradiation, the Ga-polar sample shows strong temperature dependence in the lower reverse bias region and weak temperature dependence in the higher reverse bias region. However, after irradiation with fast and thermal + fast neutrons, the entire reverse bias region shows some temperature dependence, with the temperature dependence in the higher reverse bias region increasing. The N-polar diodes, on the other hand, show temperature dependence in the low reverse bias region but less dependence in the higher reverse bias region compared to Ga-polar diodes for the pre-irradiated and fast-neutron-irradiated samples. Interestingly, the temperature dependence of *I–V* for the N-polar diode exposed to thermal + fast neutrons is very low after irradiation.

The measured reverse bias characteristics of these diodes were modeled and fitted using a combination of TE, FP emission, and

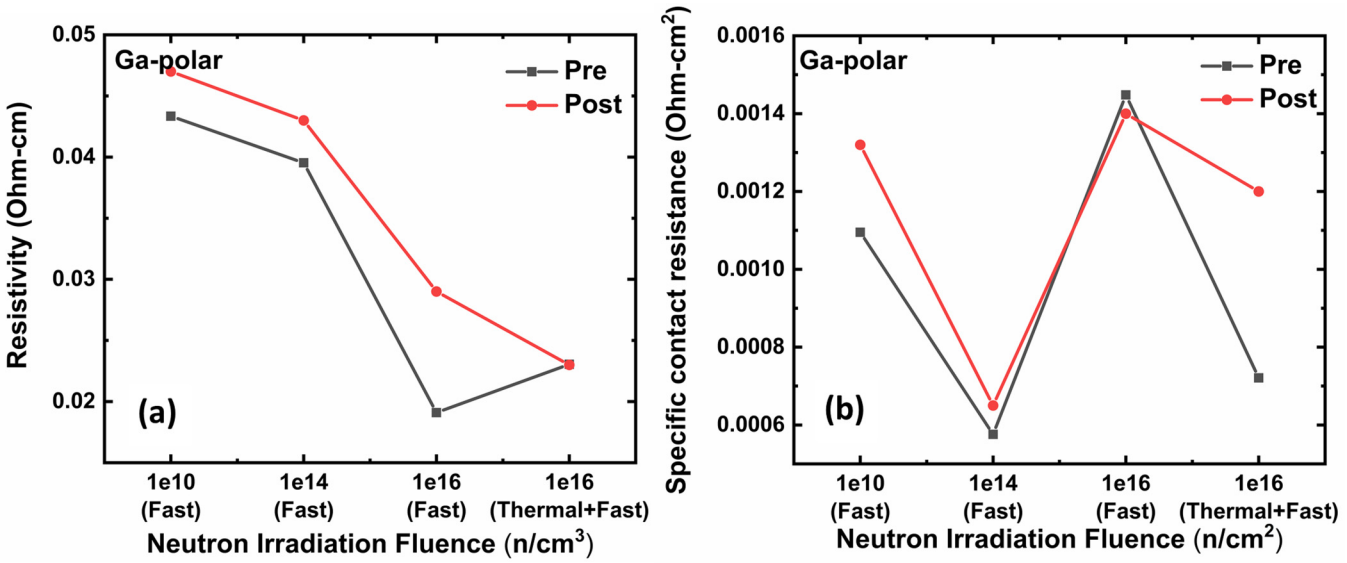

FIG. 6. Resistivity (a) and specific contact resistance (b) for Ga-polar n-type Schottky diodes (ohmic contact) pre- and post-neutron irradiation.

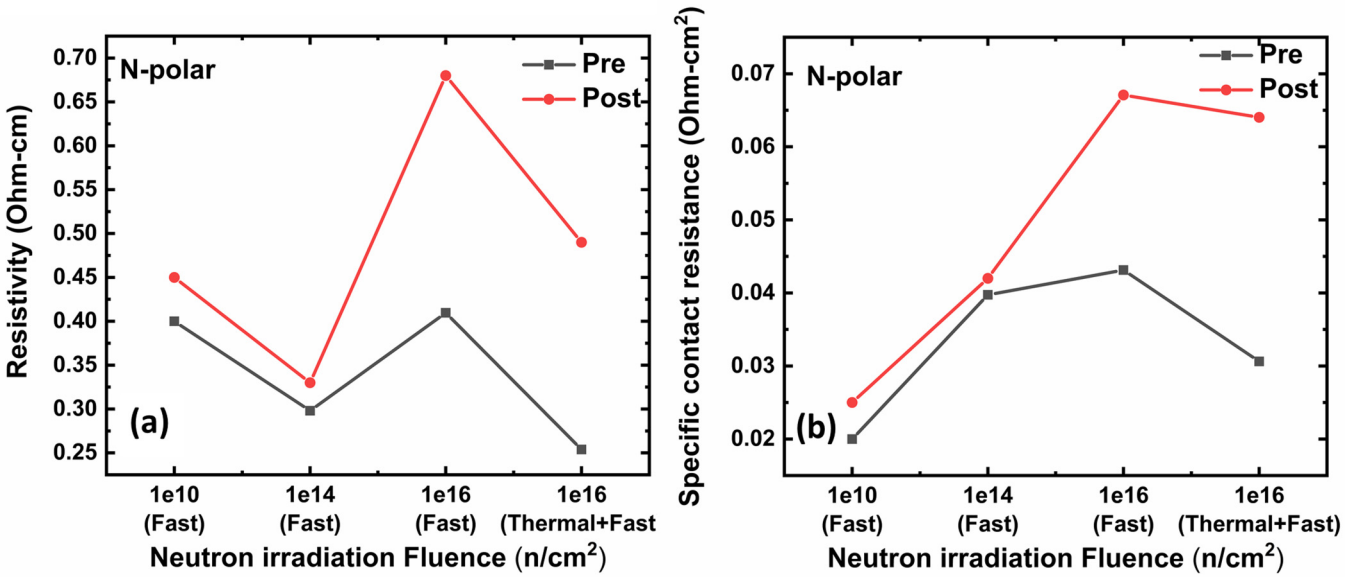

FIG. 7. Resistivity (a) and specific contact resistance (b) for N-polar n-type Schottky diodes (ohmic contact) pre- and post-neutron irradiation.

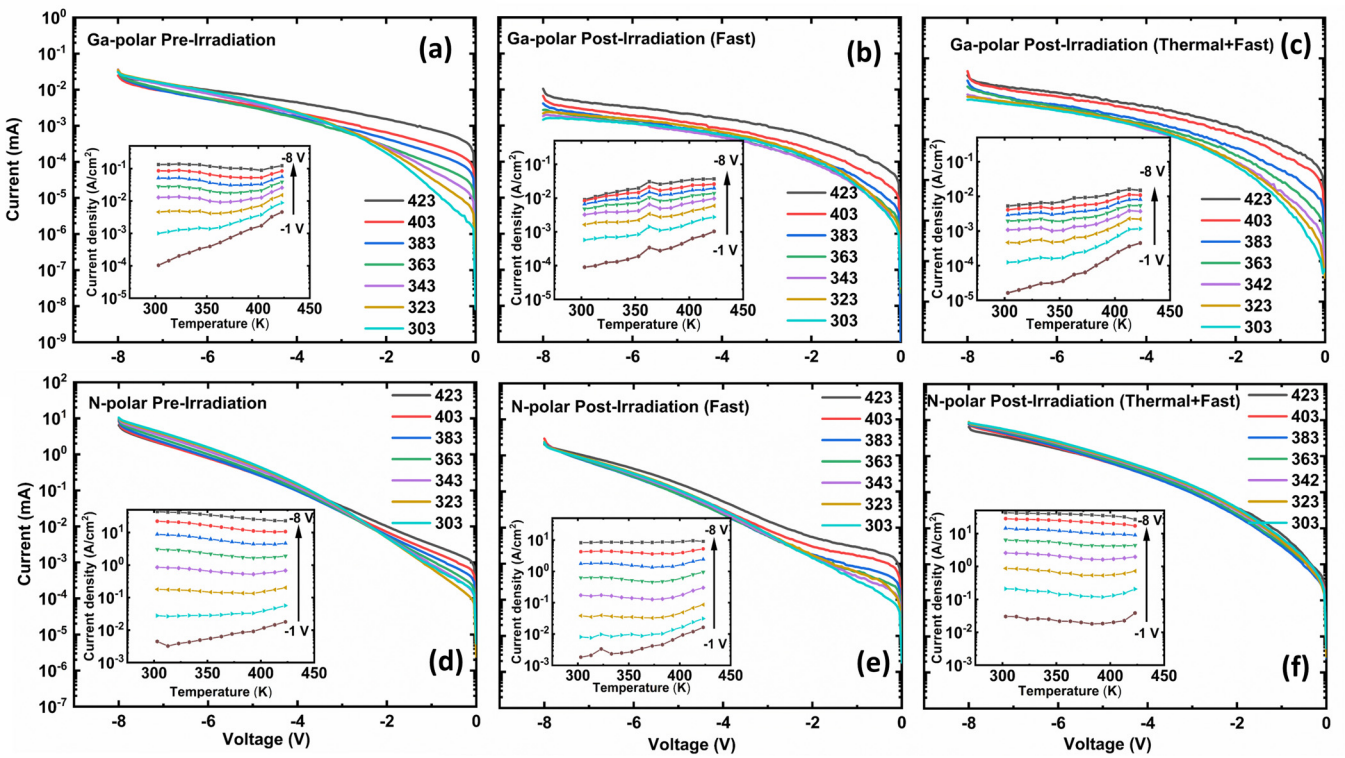

FIG. 8. Reverse current at different temperatures for Ga-polar [top row (a)–(c)] and N-polar [bottom row (d)–(f)]. The change in current density vs temperature from −1 to −8 V is shown in the inset of each graph.

FN tunneling currents ($J_{total} = J_{TE} + J_{FP} + J_{FN}$). The leakage current of these diodes is sufficiently high that the TE model cannot predict the reverse bias behavior. The extracted reverse bias current from the TE model for a Ga-polar diode is in the order of 10^{-6} (A/cm^2) and, for a N-polar diode, is in the order of 10^{-4} (A/cm^2), and both are relatively constant with reverse bias. So, the minor effect of J_{TE} was removed from J_{total} by putting the measured and extracted ideality factor and barrier height values (see Fig. 5) back into Eq. (1) and subtracting the resulting TE current from J_{total}. The remaining current density was then fit to J_{FP} and J_{FN} as briefly described below.

FP emission is related to the thermal emission of electrons from donor-like trap states to the conduction band[39] and also to the thermal emission of electrons from the Schottky metal to continuum electronic states in the barrier. The applied electric field during reverse bias induces barrier lowering for the electron emission from the trap, and these electrons result in leakage current at low reverse bias. These electrons are affected by both electric field and the temperature, so the FP current density includes both voltage and temperature. The current density corresponding to the FP emission can be expressed as follows:[40]

$$J_{FP} = CE\exp\left[\frac{-q\left(\varphi_t - \sqrt{(qE/\pi\varepsilon_i)}\right)}{kT}\right], \tag{3}$$

where C is a constant, φ_t is the effective barrier height for the electron emission from a trap state, ϵ_i is the permittivity, and E is the electric field across the barrier. To enable linear fitting to the measured I–V characteristics and extraction of the effective barrier height (φ_t), Eq. (3) can be rearranged as

$$\ln\left(\frac{J_{FP}}{E}\right) = m(T)\sqrt{E} + C(T), \tag{4}$$

where

$$m(T) = \frac{q}{kT}\sqrt{\frac{q}{\pi\varepsilon_i}},$$

$$C(T) = \frac{-q\varphi_t}{kT} + \ln(\text{Constant}). \tag{5}$$

FN tunneling is a mechanism that contributes to leakage current at high reverse bias. In this region, the high electric field and thinner barrier allow carriers to tunnel through the barrier.[39] Therefore, the FN tunneling model was used in the higher reverse-bias region where there was a higher electric field and weak temperature dependence. The FN tunneling current density is given by the following equation:[40]

$$J_{FN} = AE^2\exp\left(-\frac{B}{E}\right), \tag{6}$$

$$\ln\left(\frac{J_{FN}}{E^2}\right) = \ln(A) - \frac{B}{E},$$

where

$$B = \frac{8\pi\sqrt{2m_n^*(q\varphi_{eff})^3}}{3qh}, \tag{7}$$

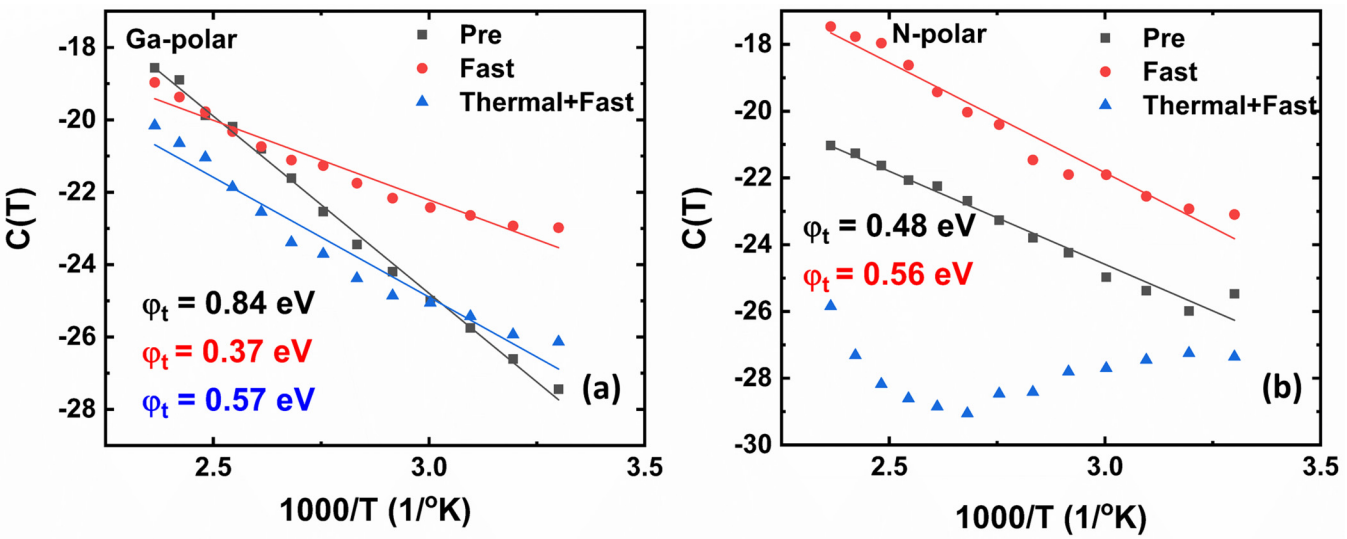

FIG. 9. Plot of $C(T)$ vs 1000/T for Ga-polar (a) and N-polar (b) for pre-irradiation, and fast and thermal + fast neutron irradiations.

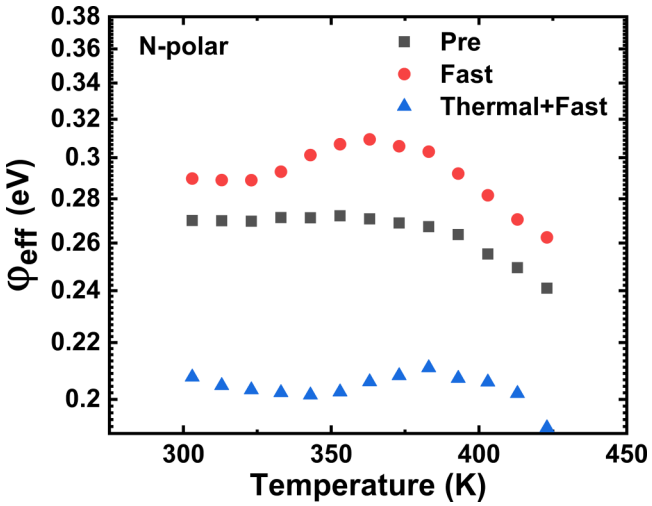

FIG. 10. Plot of the effective barrier height vs temperature for the FN tunneling emission on N-polar Schottky diodes.

where A is a constant, E is the electric field across the barrier, m_n^* is the electron effective mass, h is the Planck constant, and φ_{eff} is the effective barrier height where tunneling is initiated. Note that there is no temperature dependence for the current density in Eq. (6), so I–V characteristics when the FN mechanism dominates are expected to be relatively independent of temperature.

The changes in current density vs temperature at different reverse bias voltages suggest that J_{FP} is more dominant at reverse voltages down to −3 V, where there is stronger temperature dependence, while J_{FN} is more dominant at larger reverse voltages (≲3 V), where there is a stronger electric field and weaker temperature dependence.

The FP and FN current models can be applied to the specific reverse bias regions (as explained above) in the I–V curves. First, the FP model was used after the subtraction of J_{TE} from J_{total} in the lower reverse bias region. The plot of $\ln(J_{FP}/E)$ vs $E^{1/2}$ only shows perfect linear behavior in the low bias region, which shows that the FP model is applicable to this region. The value of $C(T)$ can be extracted for each temperature from the intercept of each plot. The extracted $C(T)$ also shows linear behavior vs temperature following Eq. (5). From the slope of the plot of $C(T)$ vs $1/T$, the value of φ_t for the un-irradiated device and for the fast and thermal + fast irradiated devices can be extracted. Figure 9 shows the plot of $C(T)$ and the extracted φ_t for both Ga-polar and N-polar diodes. For the Ga-polar diodes, the effective barrier height from the trap site is reduced from 0.84 eV pre-irradiation to 0.37 eV and 0.57 eV for fast and thermal + fast neutron irradiations, respectively. For the N-polar diode, a slight increase in the effective barrier height from 0.48 to 0.56 eV was observed after irradiation with fast neutrons. For the thermal + fast case for N-polar diodes, the FP emission model does not provide a linear fit to experimental data, as shown in Fig. 9(b), and the effective barrier height could not be extracted.

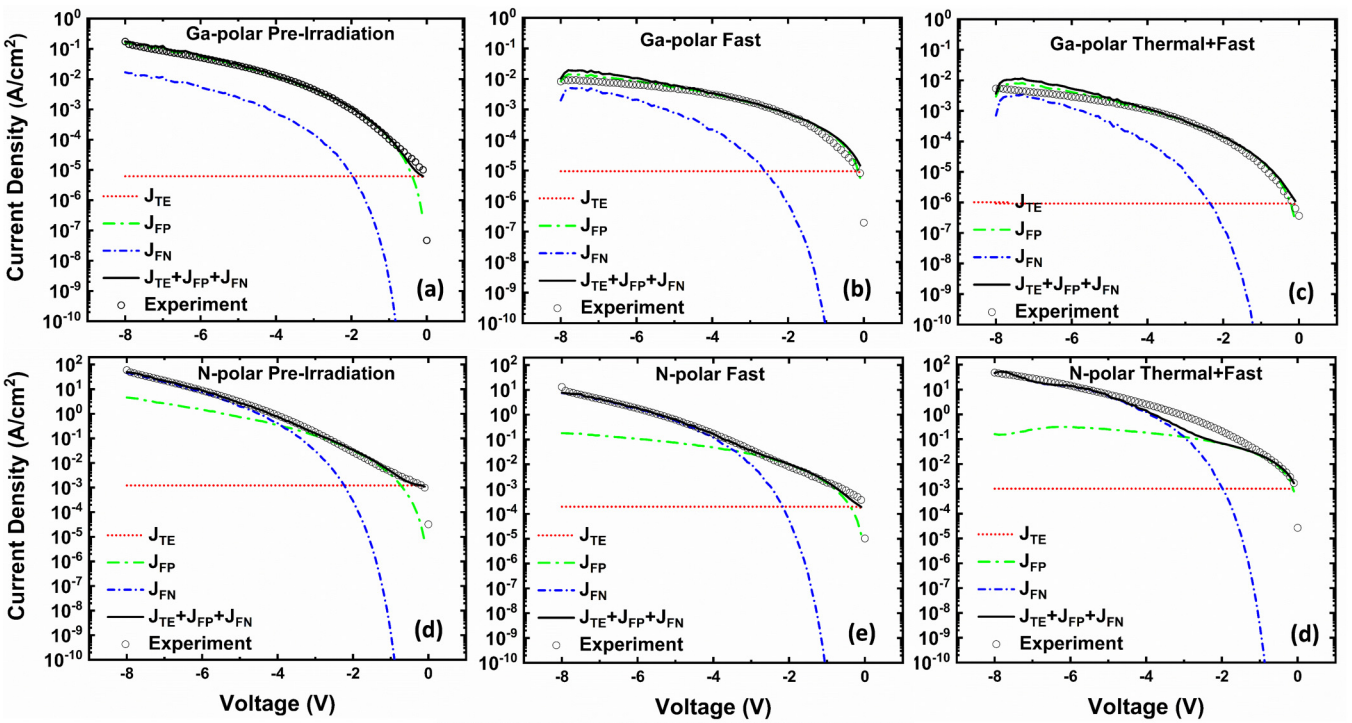

FIG. 11. Fitting result of reverse bias current density for Ga-polar [top row (a)–(c)] and N-polar (bottom row (d)–(f)] by using TE, FP emission, and FN emission models.

This suggests that the leakage current due to the FP emission is no longer dominant due to defect reconfiguration after the thermal + fast neutron irradiation. Similar behavior was previously reported in GaN heterostructures when the FP emission due to group-III vacancy complexes with dislocations disappeared after neutron radiation.[41]

Once the parameters for the FP emission were obtained from the fit, Eq. (3) was used to calculate J_{FP} for the whole reverse bias region, and then, J_{FP} was subtracted again from J_{total}, and the remaining current density is attributed to J_{FN}, with $J_{FN} = J_{total} - (J_{TE} + J_{FP})$. The plot of $\ln(J_{FN}/E^2)$ vs $1/E$ in the high-bias region also showed linear behavior (not shown here). From the slope of this plot, parameter B can be extracted and φ_{eff} can be calculated from Eq. (7). Analyzing the temperature dependent behavior of both Ga-polar and N-polar diodes shows that the FN model does not provide a linear fit to experimental data for Ga-polar devices, suggesting that leakage current based on FN tunneling is low in these devices. For the N-polar diodes, good linear fits to the FN model were obtained and the extracted φ_{eff} at different temperatures is plotted in Fig. 10. The effective tunneling barrier height shows an increase after the fast neutron irradiation, which would result in a reduction in leakage current. φ_{eff} is reduced after the thermal + fast neutron irradiation, leading to more leakage current. There is still a slight temperature dependence in extracted φ_{eff}, which suggests that the FN model cannot solely predict the leakage current behavior at higher bias voltages.

Figure 11 shows the three current density components (TE, FP, and FN) and the total current density as calculated from the models for room temperature. The experimental data are also shown. Figure 11 helps clarify the regions in which the various current components contribute to the total current. The quality of the fittings to the experimental data using the TE, FP, and FN current models is excellent for both Ga-polar and N-polar devices.

In general, the reverse leakage current can be affected from the combination of changes due to Schottky barrier height, bulk resistivity, specific contact resistance, FP emission, and FN tunneling. For the Ga-polar samples, a reduction in the barrier height for the FP emission after the neutron irradiation was observed, which suggests an increase in leakage current (inconsistent with the general leakage current reduction). The behavior of other parameters, such as SBH, bulk resistivity, specific contact resistance, and FN tunneling, after irradiation agrees with the general reduction in reverse leakage current observed in the J–V in response to both the fast and thermal + fast neutron irradiations.

For the N-polar samples, we observed an increase in SBH, bulk resistivity, and specific contact resistance for both fast and thermal + fast neutron irradiations. The barrier height for the FP emission and FN tunneling showed an increase after the fast neutron irradiation, which agrees with the I–V result for the N-polar diodes. In N-polar diodes after the thermal + fast neutron irradiation, we saw insignificant changes in leakage current [Fig. 3(d)]. In these diodes, the analysis showed both the elimination of the FP emission (corresponding to a decrease in leakage current) and a decrease in the FN tunneling barrier height (corresponding to an increase in leakage current), which suggests that the impacts from the combination of fast and thermal neutrons cancel each other and results in almost no change in the leakage current after irradiation.

IV. CONCLUSION

In this work, we investigated the impact of fast and thermal + fast neutron irradiations on the electrical performance of Ga-polar and N-polar Schottky diodes. The results show that there are fundamental differences in the electrical behavior of Schottky diodes fabricated on Ga-polar and N-polar orientations. In both Ga-polar and N-polar diodes subjected to fast and thermal + fast neutron irradiations, there was an increase in differential and series resistances after irradiation, while this increase was lower in the thermal + fast irradiation. The diode ideality factor and SBH show different behavior after fast and thermal + fast neutrons for Ga-polar and N-polar diodes. For Ga-polar diodes, the ideality factor was mostly impacted by fast neutrons, while the SBH was mostly impacted by thermal + fast neutrons. In N-polar diodes, on the contrary, the ideality factor was mostly impacted by thermal + fast, while the SBH was mostly impacted by fast neutrons. The CTLM results agree with the observed changes in the differential and series resistances and reveal that the N-polar orientation is more susceptible to bulk damage from fast neutrons. Reduction in reverse leakage current is another fundamental impact from the neutron irradiation. The Ga-polar diodes showed a larger decrease in reverse leakage current in both fast and thermal + fast neutron irradiations, while the N-polar diodes show a decrease in reverse leakage current only at a higher fluence of the fast neutron irradiation, which suggests that N-polar diodes are more tolerant to changes in reverse leakage current compared to Ga-polar diodes. TE, FP emission, and FN tunneling models were used to analyze the reverse leakage current in these diodes. On Ga-polar diodes, the effective barrier height for the electron emission from trap sites (φ_t) extracted from the FP emission model was reduced after both fast and thermal + fast neutron irradiations. Tunneling through the FN mechanism was reduced significantly after the neutron irradiation. On N-polar diodes, φ_t increased for the fast neutron irradiation, but the emission from FP disappeared after the thermal + fast neutron irradiation. The effective tunneling barrier height due to FN tunneling was also increased for the fast neutron irradiation but decreased for the thermal + fast irradiation. These observations on Ga-polar and N-polar diodes are consistent with the changes in the I–V characteristics after fast and thermal + fast neutron irradiations.

ACKNOWLEDGMENTS

The authors acknowledge funding support from the Department of Defense, Defense Threat Reduction Agency, under Grant Nos. HDTRA1-17-1-0056 (Jacob Calkins, Program Manager) and PNNL-SA-175675. We would also like to acknowledge Dr. Amanda Johnsen and Dr. Jeffery A. Geuther at Pennsylvania State University for their helpful discussions on the irradiation processes.

AUTHOR DECLARATIONS

Conflict of Interest

The authors have no conflicts to disclose.

Author Contributions

F. Mirkhosravi: Conceptualization (equal); Data curation (equal); Formal analysis (equal); Investigation (equal); Methodology (equal); Writing – original draft (equal). **A. Rashidi:** Conceptualization (supporting); Formal analysis (supporting); Writing – review & editing (supporting). **A. T. Elshafiey:** Conceptualization (equal); Investigation (equal). **J. Gallagher:** Resources (equal). **Z. Abedi:** Conceptualization (supporting); Formal analysis (supporting). **K. Ahn:** Conceptualization (supporting); Resources (supporting); Writing – review & editing (supporting). **A. Lintereur:** Conceptualization (equal); Data curation (equal); Funding acquisition (equal); Resources (equal); Writing – review & editing (equal). **E. K. Mace:** Investigation (supporting); Resources (equal). **M. A. Scarpulla:** Conceptualization (supporting); Data curation (supporting); Funding acquisition (equal); Writing – review & editing (supporting). **D. Feezell:** Conceptualization (equal); Data curation (equal); Formal analysis (supporting); Funding acquisition (lead); Resources (equal); Supervision (equal); Writing – review & editing (equal).

DATA AVAILABILITY

The data that support the findings of this study are available from the corresponding authors upon reasonable request.

REFERENCES

[1]A. Y. Polyakov, N. B. Smirnov, A. V. Govorkov, A. V. Markov, S. J. Pearton, N. G. Kolin, D. I. Merkurisov, V. M. Boiko, C.-R. Lee, and I.-H. Lee, J. Vac. Sci. Technol. B **25**, 436 (2007).

[2]S. J. Pearton, F. Ren, E. Patrick, M. E. Law, and A. Y. Polyakov, ECS J. Solid State Sci. Technol. **5**, Q35 (2016).

[3]S. J. Pearton, R. Deist, F. Ren, L. Liu, A. Y. Polyakov, and J. Kim, J. Vac. Sci. Technol. A **31**, 050801 (2013).

[4]J. Schalwig, G. Mller, O. Ambacher, and M. Stutzmann, Phys. Stat. Sol. (a) **185**, 39 (2001).

[5]J. Schalwig, G. Müller, M. Eickhoff, O. Ambacher, and M. Stutzmann, Mater. Sci. Eng. B **93**, 207 (2002).

[6]A. Ionascut-Nedelcescu, C. Carlone, A. Houdayer, H. J. von Bardeleben, J.-L. Cantin, and S. Raymond, IEEE Trans. Nucl. Sci. **49**, 2733 (2002).

[7]M. Moll, Nucl. Instrum. Methods Phys. Res. Sect. A **565**, 202 (2006).

[8]E. J. Katz, C.-H. Lin, J. Qiu, Z. Zhang, U. K. Mishra, L. Cao, and L. J. Brillson, J. Appl. Phys. **115**, 123705 (2014).

[9]A. Y. Polyakov, D.-W. Jeon, I.-H. Lee, N. B. Smirnov, A. V. Govorkov, E. A. Kozhukhova, and E. B. Yakimov, J. Appl. Phys. **113**, 083712 (2013).

[10]H. J. von Bardeleben, J. L. Cantin, U. Gerstmann, A. Scholle, S. Greulich-Weber, E. Rauls, M. Landmann, W. G. Schmidt, A. Gentils, J. Botsoa, and M. F. Barthe, Phys. Rev. Lett. **109**, 206402 (2012).

[11]B. R. Gossick, J. Appl. Phys. **30**, 1214 (1959).

[12]A. Y. Polyakov, N. B. Smirnov, A. V. Govorkov, E. A. Kozhukhova, S. J. Pearton, F. Ren, L. Liu, J. W. Johnson, W. Lim, N. G. Kolin, S. S. Veryovkin, and V. S. Ermakov, J. Vac. Sci. Technol. B **30**, 061207 (2012).

[13]C. Li and S. Subramanian, IEEE Trans. Nucl. Sci. **50**, 1998 (2003).

[14]H.-Y. Kim, J. Kim, F. Ren, and S. Jang, J. Vac. Sci. Technol. B **28**, 27 (2010).

[15]A. Y. Polyakov, N. B. Smirnov, A. V. Govorkov, N. G. Kolin, D. I. Merkurisov, V. M. Boiko, A. V. Korulin, and S. J. Pearton, J. Vac. Sci. Technol. B **28**, 608 (2010).

[16]A. Y. Polyakov, S. J. Pearton, P. Frenzer, F. Ren, L. Liu, and J. Kim, J. Mater. Chem. C **1**, 877 (2013).

[17]A. Y. Polyakov, N. B. Smirnov, A. V. Govorkov, E. A. Kozhukhova, S. J. Pearton, F. Ren, S. Y. Karpov, K. D. Shcherbachev, N. G. Kolin, and W. Lim, J. Vac. Sci. Technol. B **30**, 041209 (2012).

[18]M. Zhu, Y. Ren, L. Zhou, J. Chen, H. Guo, L. Zhu, B. Chen, L. Chen, X. Lu, and X. Zou, Microelectron. Reliab. **125**, 114345 (2021).

[19]V. N. Brudnyi, V. M. Boiko, N. G. Kolin, A. V. Kosobutsky, A. V. Korulin, P. A. Brudnyi, and V. S. Ermakov, Semicond. Sci. Technol. **33**, 095011 (2018).

[20]L. Lv, X. Yan, Y. Cao, Q. Zhu, L. Yang, X. Zhou, X. Ma, and Y. Hao, IEEE Trans. Nucl. Sci. **66**, 886 (2019).

[21]T. Fujiwara, R. Yeluri, D. Denninghoff, J. Lu, S. Keller, J. S. Speck, S. P. DenBaars, and U. K. Mishra, Appl. Phys. Express **4**, 096501 (2011).

[22]M. H. Wong, S. Keller, N. Dasgupta Sansaptak, D. J. Denninghoff, S. Kolluri, D. F. Brown, J. Lu, N. A. Fichtenbaum, E. Ahmadi, U. Singisetti, A. Chini, S. Rajan, S. P. DenBaars, J. S. Speck, and U. K. Mishra, Semicond. Sci. Technol. **28**, 074009 (2013).

[23]F. Akyol, D. N. Nath, S. Krishnamoorthy, P. S. Park, and S. Rajan, Appl. Phys. Lett. **100**, 111118 (2012).

[24]M. H. Wong, Y. Pei, T. Palacios, L. Shen, A. Chakraborty, L. S. McCarthy, S. Keller, S. P. DenBaars, J. S. Speck, and U. K. Mishra, Appl. Phys. Lett. **91**, 232103 (2007).

[25]Z. Q. Li, M. Lestradet, Y. G. Xiao, and S. Li, Phys. Stat. Sol. A **208**, 928 (2011).

[26]S. Bharadwaj, J. Miller, K. Lee, J. Lederman, M. Siekacz, H. Xing, D. Jena, C. Skierbiszewski, and H. Turski, Opt. Express **28**, 4489 (2020).

[27]B. L. VanMil, H. Guo, L. J. Holbert, K. Lee, T. H. Myers, T. Liu, and D. Korakakis, J. Vac. Sci. Technol. B **22**, 2149 (2004).

[28]R. Togashi, T. Kamoshita, H. Adachi, H. Murakami, Y. Kumagai, and A. Koukitu, Phys. Stat. Sol. C **6**, S372 (2009).

[29]F. Mirkhosravi, A. Rashidi, J. Gallagher, M. Monavarian, A. Aragon, K. Ahn, Y. K. Ooi, A. Lintereur, E. K. Mace, M. A. Scarpulla, and D. Feezell, AIP Adv. **11**, 025009 (2021).

[30]H.-Y. Kim, F. Ren, S. J. Pearton, and J. Kim, Electrochem. Solid State Lett. **12**, H173 (2009).

[31]P. Reddy, B. Sarkar, F. Kaess, M. Gerhold, E. Kohn, R. Collazo, and Z. Sitar, Appl. Phys. Lett. **110**, 011603 (2017).

[32]H. Yamada, H. Chonan, T. Takahashi, and M. Shimizu, Phys. Stat. Sol. A **215**, 1700362 (2018).

[33]B. S. Eller, J. Yang, and R. J. Nemanich, J. Electron. Mater. **43**, 4560 (2014).

[34]U. Karrer, O. Ambacher, and M. Stutzmann, Appl. Phys. Lett. **77**, 2012 (2000).

[35]J. Yang, B. S. Eller, and R. J. Nemanich, J. Appl. Phys. **116**, 123702 (2014).

[36]R. T. Tung, Mater. Sci. Eng., R **35**, 1 (2001).

[37]W. Mtangi, P. J. J. van Rensburg, M. Diale, F. D. Auret, C. Nyamhere, J. M. Nel, and A. Chawanda, Mater. Sci. Eng. B **1**, 171 (2010).

[38]D. K. Schroder, *Semiconductor Material and Device Characterization*, 3rd ed. (IEEE Press, Piscataway, NJ, 2006).

[39]J. Ren, W. Mou, L. Zhao, D. Yan, Z. Yu, G. Yang, S. Xiao, and X. Gu, IEEE Trans. Electron Devices **64**, 407 (2017).

[40]S. M. Sze, K. K. Ng, and Y. Li, *Physics of Semiconductor Devices*, 4th ed. (Wiley, Hoboken, NJ, 2021).

[41]R. Wang, J. Xu, S. Zhang, Y. Zhang, P. Zheng, Z. Cheng, L. Zhang, F.-X. Chen, X. Tong, Y. Zhang, and W. Tan, J. Mater. Chem. C **9**, 3177 (2021).